A novel mathematical approach for the understanding and optimization of two-phase partitioning bioreactors devoted to air pollution control

Antonio D. Dorado[2], Eric Dumont[3], Raúl Muñoz[1], Guillermo Quijano[1*]

1. University of Valladolid. Department of Chemical Engineering and Environmental Technology. Dr. Mergelina s/n, 47011 Valladolid, Spain. Phone: +34983186424, Fax: +34983423013.

2. Universitat Politècnica de Catalunya, Department of Mining Engineering and Natural Resources. Av. Bases de Manresa 61-73, Manresa, Spain.

3. UMR CNRS 6144 GEPEA, École des Mines de Nantes, 4 rue Alfred Kastler, BP 20722, 44307 Nantes Cedex 03, France.

[*]Corresponding author, email: gquijano@iq.uva.es

Abstract

Two-phase partitioning bioreactors (TPPBs) support the removal of volatile organic compounds (VOCs) from contaminated gaseous emissions at unprecedented rates and concentrations. TPPBs are biological multiphase systems provided with a non-aqueous phase (NAP) with high affinity for the target VOC. Although modeling of TPPBs is a research field that has rapidly evolved, recent experimental findings such as the direct VOC uptake from liquid NAPs and the quantification of simultaneous partial mass transfer coefficients have not been incorporated yet in a comprehensive mathematical description. In this work, a mathematical description of TPPBs, including continuous aqueous phase renewal and potential VOC uptake directly from the NAP, was developed. Model simulations indicated that TPPB performance can be enhanced by improving the partial mass transfer coefficient between the gas and the NAP (by increasing the contact between the gas and the NAP). The model also showed that microorganisms with half-saturation constants < 5 g m^{-3} and ability to take up VOC directly from the NAP can boost significantly TPPB performance. The present modeling platform was tested against experimental data from literature for methane, hexane and dichloromethane and no parameter fitting was carried out.

Keywords: Biological gas treatment; mathematical modeling; two-phase partitioning bioreactors; volatile organic compounds.

1. Introduction

Two-phase partitioning bioreactors (TPPBs) devoted to air pollution control are multiphase systems based on the addition into a biological process of a non-aqueous phase (NAP) with high affinity for target gaseous pollutants [1]. TPPBs support the biological removal of volatile organic compounds (VOCs) from contaminated gaseous streams at unprecedented rates and concentrations [2,3]. The presence of the NAP improves the transfer of hydrophobic VOCs from the gas to the microorganisms and overcomes operational issues induced by the toxicity of some hydrophilic VOCs [4]. Moreover, most NAPs used for TPPB implementation show a high affinity for O_2 and consequently, the increase in the VOC mass transfer in TPPBs is concomitant with an increase in the O_2 transfer rate, enhancing the opportunities for complete VOC mineralization [5,6]. Thus, the VOC biodegradation performance in TPPBs is often superior to that recorded in conventional biological gas treatment systems [7,8].

Modeling of TPPBs is a research field that has rapidly evolved, bringing key insights on the mechanisms underlying VOC biodegradation and identifying relevant experimental research niches for the optimization of this technology platform. For instance, Cruickshank et al. [9] described the strong impact of O_2 limitation on the performance of TPPBs by means of a comprehensive mathematical model. The key role of the biological kinetic parameters (particularly the VOC half-saturation constant K_S) on the performance of TPPBs was anticipated by the mathematical description proposed by Fazaelipoor [10]. Likewise, the occurrence of a direct VOC uptake in the NAP was early proposed in the mathematical description of the benzene vapor removal in TPPBs by Nielsen et al. [11,12] The impact of the NAP addition on the VOC absorption in TPPBs has been better understood from the modeling approach of Dumont et al. [13,14]. Mechanistic models for TPPBs using solid NAPs are also available in the literature [15]. However,

although such models can give useful information they cannot be directly applied to TPPBs using liquid NAPs.

The increased pace of experimental studies in TPPBs conducted in the past 10 years has significantly expanded our understanding of the complex mass transfer phenomena and substrate uptake mechanisms, which constitute the fundamental processes governing the performance of these multiphase systems [5,8]. Recent experimental findings confirmed the direct VOC uptake from liquid NAPs in some instances, opening new possibilities for the development of high-performance TPPBs [16,17]. Moreover, the quantification of simultaneous mass transfer pathways established in TPPBs has been recently reported for O_2 by determining partial mass transfer coefficients [18]. However, this fundamental knowledge recently gained in microbiology and mass transfer aspects has not been incorporated yet in a comprehensive mathematical description of TPPBs.

In this work, a novel mathematical description of TPPBs accounting for the last experimental findings reported in the literature was proposed. A comprehensive description of the complex mass transfer phenomena occurring simultaneously in TPPBs was done by means of partial mass transfer coefficients for both VOC and O_2. The model also features potential VOC/O_2 uptake in the NAP and continuous aqueous phase renewal (usually done to avoid nutrients limitations and remove inhibitory metabolites). Finally, the results obtained from a sensitivity analysis and model simulations were compared with recent experimental data, critical research niches being identified and discussed.

2. Mathematical model

2.1 Two-phase partitioning bioreactor

The TPPB considered in this work was a standard stirred tank reactor operated with silicone oil as a NAP. Silicone oil was selected since it is the most investigated NAP in TPPBs devoted to air pollution control [1,5]. In addition, silicone oil is, to the best of our knowledge, the only liquid NAP so far reported that is fully biocompatible, water immiscible and non-biodegradable [19,20]. The gas phase consisted of an air stream laden with a single VOC continuously introduced to the reactor, while the aqueous phase consisted of a diluted nutrients solution renewed at a constant flow rate. The mathematical model was based on the following parameters: liquid phase composition, gas and water flow rates, VOC and O_2 concentrations (in gas, NAP and water), VOC and O_2 partition between phases, mass transfer coefficients between phases and kinetics of microbial growth. A constant temperature of 25°C was considered for model simulations (the kinetic, mass transfer and partition coefficients used were obtained at this temperature).

2.2 Model assumptions

The following key assumptions were made in order to provide a standardized modeling framework: (i) the TPPB was operated under complete mixing conditions; (ii) the microbial kinetic parameters remained the same regardless of the liquid phase the microorganisms grow; (iii) the specific microbial decay rate accounted for 10% of the maximum specific growth rate [21]; (iv) the gas holdup was assumed to remain at 10% relative to the total working volume regardless of the NAP percentage [22,23]; and (v) the TPPB performance was not affected by the dynamic viscosity of the NAP at oil percentages ranging 10-20% (the hydrodynamic conditions were not taken into account in the model).

2.3 Model equations

The mathematical model was based on mass balances for biomass in both NAP and aqueous phase as well as on mass balances for VOC and O_2 in the gas, NAP and aqueous phase. A double Monod-type equation was used to describe the specific microbial growth rate in both the aqueous phase (μ_W) and the NAP (μ_{NAP}) in order to account for the effect of O_2 limitations:

$$\mu_W = \mu_{\max}\left(\frac{C_W}{K_S + C_W}\right)\left(\frac{O_{2W}}{K_O + O_{2W}}\right) - \mu_d \quad (1)$$

$$\mu_{NAP} = \mu_{\max}\left(\frac{C_{NAP}}{K_S + C_{NAP}}\right)\left(\frac{O_{2NAP}}{K_O + O_{2NAP}}\right) - \mu_d \quad (2)$$

Substrate inhibition was not considered in the present work since TPPBs are mainly used for the removal of very hydrophobic VOCs at low loading rates (conditions commonly resulting in mass transfer limitations). However, inhibition can be easily incorporated in the model by using a Haldane-Andrews type kinetics.

The balance for biomass in the aqueous phase was described by:

$$\frac{dX_W}{dt} = \left[\mu_{\max}\left(\frac{C_W}{K_S + C_W}\right)\left(\frac{O_{2W}}{K_O + O_{2W}}\right) - \mu_d\right]X_W - \frac{Q}{(1-\phi_{NAP}-\phi_G)V_T}X_W \quad (3)$$

Likewise, the balance for biomass in the NAP was described as:

$$\frac{dX_{NAP}}{dt} = \left[\mu_{\max}\left(\frac{C_{NAP}}{K_S + C_{NAP}}\right)\left(\frac{O_{2NAP}}{K_O + O_{2NAP}}\right) - \mu_d\right]X_{NAP} - \frac{Q_N}{(1-\phi_W-\phi_G)V_T}X_{NAP} \quad (4)$$

The aqueous phase and the NAP are continuously renewed to provide nutrients, remove potentially inhibitory metabolites and avoid excessive biomass accumulation. However, in the studies used for validating the model of the present work any author indicates NAP renovation due to the relative

short length of the experiments (lower than 2 months). In any of the TPBBs performed in stirred tank have been reported uncontrolled or planned losses of NAP. Accordingly, the purge term of NAP were simplified (Q_N=0) for these specific cases.

The need for water renewal during VOC removal in TPPBs has been consistently pointed out by several authors [16,17,23]. On the other hand, the mass balance for VOC in the gas phase was described as follows:

$$\frac{dC_G}{dt} = \frac{F}{V_T}\frac{(C_{Gin} - C_G)}{(1-\phi_W-\phi_{NAP})} - \left(k_L^{G/W}a\right)_{VOC}\left(\frac{C_G}{K_{G/W}^{VOC}} - C_W\right)\frac{(1-\phi_G-\phi_{NAP})}{(1-\phi_W-\phi_{NAP})} - \\ - \left(k_L^{G/NAP}a\right)_{VOC}\left(\frac{C_G}{K_{G/NAP}^{VOC}} - C_{NAP}\right)\frac{(1-\phi_G-\phi_W)}{(1-\phi_W-\phi_{NAP})} \quad (5)$$

The rate of VOC accumulation in the aqueous phase and in the NAP was described by Equations 6 and 7, respectively:

$$\frac{dC_W}{dt} = \left(k_L^{G/W}a\right)_{VOC}\left(\frac{C_G}{K_{G/W}^{VOC}} - C_W\right) + \left(k_L^{NAP/W}a\right)_{VOC}\left(\frac{C_{NAP}}{K_{NAP/W}^{VOC}} - C_W\right) - \\ - \frac{\mu_W}{Y_{X/S}}X_W - \frac{Q}{(1-\phi_G-\phi_{NAP})V_T}C_W \quad (6)$$

$$\frac{dC_{NAP}}{dt} = \left(k_L^{G/NAP}a\right)_{VOC}\left(\frac{C_G}{K_{G/NAP}^{VOC}} - C_{NAP}\right) - \\ - \left(k_L^{NAP/W}a\right)_{VOC}\left(\frac{C_{NAP}}{K_{NAP/W}^{VOC}} - C_W\right)\frac{(1-\phi_G-\phi_{NAP})}{(1-\phi_G-\phi_W)} - \frac{\mu_{NAP}}{Y_{X/S}}X_{NAP} \quad (7)$$

The balance for O_2 in the gas phase was described using Equation 8:

$$\frac{dO_{2G}}{dt} = \frac{F}{V_T}\frac{(O_{2Gin} - O_{2G})}{(1-\phi_W-\phi_{NAP})} - \left(k_L^{G/W}a\right)_{O_2}\left(\frac{O_{2G}}{K_{G/W}^{O_2}} - O_{2W}\right)\frac{(1-\phi_G-\phi_{NAP})}{(1-\phi_W-\phi_{NAP})} - \\ - \left(k_L^{G/NAP}a\right)_{O_2}\left(\frac{O_{2G}}{K_{G/NAP}^{O_2}} - O_{2NAP}\right)\frac{(1-\phi_G-\phi_W)}{(1-\phi_W-\phi_{NAP})} \quad (8)$$

The rate of O_2 accumulation in the aqueous phase and in the NAP was described by Equations 9 and 10, respectively:

$$\frac{dO_{2W}}{dt} = \left(k_L^{G/W} a\right)_{O_2}\left(\frac{O_{2G}}{K_{G/W}^{O_2}} - O_{2W}\right) + \left(k_L^{NAP/W} a\right)_{O_2}\left(\frac{O_{2NAP}}{K_{NAP/W}^{O_2}} - O_{2W}\right) + \\ + \frac{Q}{\left(1-\phi_G-\phi_{NAP}\right)V_T}\left(O_{2Win} - O_{2W}\right) - \frac{\mu_W}{Y_{X/O_2}} X_W \quad (9)$$

$$\frac{dO_{2NAP}}{dt} = \left(k_L^{G/NAP} a\right)_{O_2}\left(\frac{O_{2G}}{K_{G/NAP}^{O_2}} - O_{2NAP}\right) - \\ - \left(k_L^{NAP/W} a\right)_{O_2}\left(\frac{O_{2NAP}}{K_{NAP/W}^{O_2}} - O_{2W}\right)\frac{\left(1-\phi_G-\phi_{NAP}\right)}{\left(1-\phi_G-\phi_W\right)} - \frac{\mu_{NAP}}{Y_{X/O_2}} X_{NAP} \quad (10)$$

2.4 Model solution

The resulting set of ordinary differential equations (Equations 3-10) was solved using MATLAB® in a home-made modeling environment. A variable order method based on the numerical differentiation formulas (NDFs) was used for solving Stiff differential equations. The maximum time step used in the numerical solution routine was set at 1 h. Despite the model was solved for dynamic conditions, only steady state removal rates were considered to perform comparisons.

3. Data compilation

3.1 Kinetic, partition and mass transfer parameters

A literature review was carried out in order to compile the available experimental data on kinetic, partition and mass transfer parameters required by the mathematical model here proposed. This step was very important to set the typical values for the above referred parameters and to perform

both the sensitivity analysis and the subsequent model validation. Table 1 summarizes the kinetic and stoichiometric parameters reported for aerobic VOC-degrading microorganisms. It must be stressed that TPPBs are mainly used for the removal of hydrophobic and moderately hydrophilic VOCs such as hexane, methane, BTEX or dichloromethane [5,13]. However, a highly hydrophilic VOC (acetone) was also considered in order to investigate the performance of TPPBs under a wide variety of VOC hydrophobicities. When the complete kinetic parameter dataset for a target VOC was not available in the literature, typical values for heterotrophic bacteria were considered according to Bailey and Ollis [25] (K_O=0.288 g m^{-3} and $Y_{X/O2}$ = 0.558 g g^{-1}). Moreover, when more than one kinetic or stoichiometric parameter was found for a particular VOC the mean value was used for model simulations. From Table 1, it can be observed that μ_{max}, K_S and $Y_{X/S}$ were available for most target VOCs. Nevertheless, there is a lack of experimental values for K_O and $Y_{X/O2}$ regardless of the VOC. Hexane was the VOC with less reported kinetic data in the literature likely due its low water solubility (dimensionless Henry's law constant of 70), which severely hinders the determination of kinetic biodegradation parameters. Table 2 summarizes the partition parameters required by the mathematical model. Interestingly, there is abundant literature on VOC partitioning data in TPPBs, which can be explained by the fact that the NAP affinity towards the target VOC has been regarded as one of the most important design parameters for TPPBs devoted to air pollution control [3,13,22].

<Table 1>

<Table 2>

3.2 Estimation of partial mass transfer coefficients for VOCs

Unlike the case of the VOC partition data, experimental data on partial mass transfer coefficients reported in the literature are very scarce. To the best of our knowledge, partial mass transfer

coefficients have been experimentally determined only for O_2, while no experimental data have been reported for VOCs in TPPBs. In the present modeling study, experimental values of the partial mass transfer coefficients were required to perform simulations and comparisons among the available VOC removal studies in TPPBs. Therefore, all the $\left(k_L^{i/j}a\right)_{VOC}$ values were estimated from experimental $\left(k_L^{i/j}a\right)_{O2}$ data available in the literature. According to Yu et al. [40] the mass transfer coefficient of any gaseous compound across a liquid film can be estimated as a function of the molecular volume at its boiling point (V_m). The correlation for complete mixing conditions can be written as:

$$k_L a \propto \left(1/V_m\right)^{0.4} \tag{11}$$

These authors demonstrated that the mass transfer coefficient of a given gas pollutant (k_La_X) can be estimated from the coefficient of a reference gas (k_La_{ref}) experimentally determined in the same reactor under the same operating conditions as follows:

$$\frac{k_L a_X}{k_L a_{ref}} = \frac{\left(1/V_{m,X}\right)^{0.4}}{\left(1/V_{m,ref}\right)^{0.4}} \tag{12}$$

Thus, Equation 12 can be applied to estimate the k_La values of target VOCs from experimentally-determined k_La data for oxygen. The V_m values used for k_La_X estimation were 64.8, 106.3, 130.7, 56.3 and 39.0 mL mol^{-1} for acetone, toluene, hexane, dichloromethane and methane, respectively, while the V_m value for oxygen was 25.6 mL mol^{-1} [41-44]. Equation 12 has been successfully used to estimate the mass transfer coefficients of methane, NH_3, H_2S, toluene and hexane from experimental O_2 mass transfer coefficients [40,45]. Table 3 summarizes the experimental O_2 mass transfer coefficients and the estimated coefficients for several target VOCs. The experimental mass

transfer data for O_2 was available for a wide range of NAP percentages (from 0 to 50% v/v), which allowed the estimation of VOC mass transfer coefficients under such varied NAP percentages.

<Table 3>

4. Results and discussion

4.1 Model validation

The mathematical model developed was used to predict the RE reported in several case studies. The operational conditions used in these works (e.g. V_T, F, Q, ϕ_{NAP}) together with the required kinetic, stoichiometric and mass transfer parameters (Tables 1-3) were set in the model. Table 4 summarizes the operational conditions and the removal efficiency (RE defined as the percentage of inlet pollutant removed) recorded in the works used for model validation. Only experimental studies using silicone oil as a NAP were considered since all experimental partition coefficients required by the model ($K_{i/j}^{VOC}$ and $K_{i/j}^{O_2}$) were available in the literature. The RE of the control systems without silicone oil addition was accurately predicted by the model in three of the six experimental studies considered (Fig. 1A). Bailon et al. [35] evaluated dichloromethane removal at loading rates of 100 and 300 g m^{-3} h^{-1}. In this particular study, while the model yielded an accurate RE prediction for the first loading rate (case A), it overestimated the RE obtained at a loading rate of 300 g m^{-3} h^{-1} (case B). Such overestimation was attributed to the fact that dichloromethane is a toxic and relatively water soluble VOC (~700 and ~300 times more soluble in water compared with hexane and methane, respectively). This, together with the fact that 300 g m^{-3} h^{-1} is an unusually high loading rate, suggested that the TPPB was operated under inhibitory conditions. Therefore, the lack of substrate inhibition kinetics (e.g. Haldane-Andrews type kinetics) in the model likely resulted in an overestimated RE.

<Table 4>

<Figure 1>

The model underestimation of the REs reported by Rocha-Rios et al. [23] and Muñoz et al. [46] might be due to the fact that $\left(k_L^{G/W}a\right)_{VOC}$ was estimated from $\left(k_L^{G/W}a\right)_{O2}$, the latter being obtained at an agitation speed of 300 rpm [18], while the agitation speeds used by these authors were 800 and 400 ppm, respectively. This hypothesis was supported by the fact that the REs reported by Hernandez et al. [16] and Muñoz et al. [17] for their control systems operated at an agitation speed of 300 rpm were accurately predicted by the model. Knowing other operational factors affecting the mass transfer coefficient estimation such as geometry of the impellers, interfacial tension, mixture rheology or temperature, would let a more accurately estimation of this parameter if data would have been available.

Figure 1B shows the experimental RE values and the model predictions assuming no biomass growth in the NAP (and therefore no VOC uptake in the NAP). For this purpose, the model simulations were performed without biomass in the NAP (X_{NAP}= 0). It was observed that the model predicted accurately the RE of dichloromethane [35], which was the most hydrophilic VOC from the pool of pollutants studied. However, the model predictions largely underestimated the RE reported for hydrophobic VOCs (hexane and methane). Interestingly, the model underestimated the RE reported in those works operating the TPPBs at 300 rpm [16,17], which was the same agitation speed used for the experimental determination of the $\left(k_L^{i/j}a\right)_{O2}$ values. Therefore, the poor model performance could not be completely attributed to $\left(k_L^{i/j}a\right)_{VOC}$ underestimation.

Figure 1C shows the model results assuming biomass growth in the NAP (initial X_{NAP}= 1 g m^{-3}). It was observed that this assumption drastically improved the model performance. From the five experimental works considered for model validation, two of them confirmed the VOC uptake in the NAP [16,17]. Therefore, the fact that the model performed significantly better assuming VOC uptake in the NAP strongly suggested that even when biomass growth in the NAP was not

considered in the experimental works it occurred. It can be hypothesized that the amount of biomass able to take up VOC from the NAP varies with the characteristics of the microbial community and the operational conditions (e.g. mixing characteristics, NAP dispersion degree). Therefore, the mathematical model predictions can still be improved if the X_{NAP} value is optimized for each experimental work. In this regard, the experimental quantification of biomass concentration in the NAP seems to be feasible (e.g. measuring protein content in the organic phase), enabling a better model performance and improving the model-based design and operation of TPPBs.

Another critical research niche is the experimental determination of the partial VOC mass transfer coefficients. In this regard, it can be expected a better model performance by using experimental $\left(k_L^{i/j}a\right)_{VOC}$ values rather than using estimated values. From the sensitivity analysis, it was clear that $\left(k_L^{G/NAP}a\right)_{VOC}$ was the coefficient with the highest impact on the VOC removal performance. Figure 2 shows how changes in $\left(k_L^{G/NAP}a\right)_{VOC}$ impact on the RE predicted by the model. It was observed that the model predictions improved as $\left(k_L^{G/NAP}a\right)_{VOC}$ increases, this being particularly clear for hydrophobic VOCs. It is worth noting that increases higher than 50% in $\left(k_L^{G/NAP}a\right)_{VOC}$ are required to predict adequately the RE recorded by Muñoz et al. [17,46] and Rocha-Rios et al. [23], which highlights the relevance of the experimental determination of the partial mass transfer coefficients for the VOC.

<Figure 2>

4.2 Sensitivity analysis

A sensitivity analysis was performed in order to identify the parameters exhibiting the highest influence on model predictions. The analysis was performed using typical operational conditions

for TPPBs. The VOC removal efficiency (RE) was used as the performance state variable according to Equation 13:

$$RE\ (\%) = \frac{C_{Gin} - C_G}{C_{Gin}} \times 100 \quad (13)$$

Model sensitivity was assessed by increasing and decreasing the values of the parameters and predicting the corresponding relative change in RE. Thus, process parameters were varied from 0.2 to 5 times relative to the initial values given in Table 5. Toluene was selected as the reference VOC to set the initial parameters for the sensitivity analysis since it is neither extremely hydrophobic nor hydrophilic [5]. The results obtained from the sensitivity analysis were classified by type of parameters (e.g. operational, mass transfer, partition and kinetic parameters). The gas flow rate (F) as well as the NAP fraction (ϕ_{NAP}) were the most relevant operational parameters in terms of RE sensitivity (Fig. 3A). The gas flow rate is a parameter related with the contact time between the pollutant-laden gas stream and the liquid phases. Thus, an increase in the gas flow rate will result in a decrease of the gas contact time with both water and NAP, which in turn would result in a lower VOC removal performance. Indeed, the sensitivity analysis showed a decrease of 22% in the relative RE when doubling the initial gas flow rate. Conversely, a reduction of the gas flow rate by a factor of 5 would entail an increase of 20% in the relative RE.

<Table 5>

<Figure 3>

Moreover, the high sensitivity of the model towards variations in ϕ_{NAP} was in agreement with the literature. Several experimental works concluded that the NAP fraction is often one of the most important operation parameters in TPPBs [13,18,47]. The sensitivity analysis also showed that an

increase in C_{Gin} will produce a significant increase in the RE. This indicates that under the similar operating conditions, the RE of a given VOC will increase with the inlet pollutant concentration. Such enhancement can be attributed to an increased VOC concentration gradient between the gas and the liquid phases which finally improves the mass transfer performance in the TPPB and consequently also the microbial kinetics.

On the other hand, the predicted RE showed a higher sensitivity towards the gas-to-NAP transfer coefficient for the VOC, $\left(k_L^{G/NAP}a\right)_{VOC}$, compared to those coefficients defining the transfer among the rest of phases (G/W and NAP/W) (Fig. 3B). Interestingly, the gas-to-NAP transfer coefficient for O_2 showed a marginal impact on the relative RE, which highlights the fact that the VOC transfer between the gas phase and the NAP is the key mass transport mechanism in the TPPB. These results strongly suggested that the VOC removal performance can be enhanced if the contact between the gas and the NAP is promoted. This observation was consistent with the hydrophobic character of toluene (highly affine for silicone oil) and underlines the relevance of the accurate characterization of the mass transport parameters in order to describe and predict correctly the RE recorded in TPPBs. Therefore, efforts on the experimental determination of the partial mass transfer coefficients must still be done.

The VOC equilibrium between the gas and the NAP ($K_{G/NAP}^{VOC}$) was by far the most relevant partition parameter in the model (Fig. 3C). This result highlights the relevance of the NAP selection in order to implement TPPBs with a NAP highly affine for the target VOC. Thus, VOC-NAP pairs yielding $K_{G/NAP}^{VOC}$ values << 1 should be selected, which was in agreement with many experimental works concluding that $K_{G/NAP}^{VOC}$ is one of the most critical parameters in TPPB design [13,36,48,49]. The model also showed a high sensitivity towards a decrease in $K_{G/W}^{VOC}$ values. This means that a higher and positive impact on RE will be observed as the VOC become more hydrophilic, while a lower

and negative impact on RE will be observed as the VOC become hydrophobic. These results were in agreement with the literature regarding TPPBs are systems particularly suitable for the treatment of hydrophobic VOCs [5]. Thus, the RE in a TPPB will not dramatically decrease when increasing the VOC hydrophobicity (high $K_{G/W}^{VOC}$ values) as would occur in a conventional aqueous-based bioreactor. It must be also remarked that the O_2 partition coefficients ($K_{i/j}^{O_2}$) showed a marginal impact on RE compared with $K_{G/NAP}^{VOC}$ and $K_{G/W}^{VOC}$.

The maximum specific growth rate (μ_{max}) was the most relevant parameter in terms of RE sensitivity, its impact on TPPB performance being much more important at lower values (Fig. 3D). It is worth noting that a marginal impact of μ_{max} on RE was observed for values ranging 0.13-0.67 h^{-1} (variations in RE< 5%). Interestingly, μ_{max} values within this range are common for aerobic heterotrophic microorganisms. Nevertheless, μ_{max} values lower than 0.13 h^{-1} have been indeed reported for some VOCs such as methane, dichloromethane or acetone (Table 1). Therefore, experimental efforts must be made in order to isolate microorganisms able to degrade these VOCs supporting μ_{max} values > 0.13 h^{-1}. On the other hand, μ_{max} values > 0.67 h^{-1} impacted RE in a lesser extent since the limiting step of the process shifts to mass transfer aspects. The sensitivity analysis also indicated that the half-saturation constant for the VOC (K_S) has an important effect on RE at low values (e.g. K_S < 5 g m^{-3}), corresponding to microorganisms supporting a high affinity towards the VOC. These results were in agreement with Fazaelipoor [10], who highlighted the relevance of low K_S values for increasing TPPB performance. The sensitivity analysis here performed under the current operational conditions clearly identified VOC mass transfer rather than biological activity as the main limitation of the system. Overall, the outputs of the mathematical model were in agreement with the experimental findings so far reported in the literature.

5. Conclusions

An innovative mathematical description of TPPBs based on partial mass transfer coefficients and accounting for VOC and O_2 uptake directly from the NAP was developed. The model simulations indicated that the most effective way to improve TPPB performance is increasing the $\left(k_L^{G/NAP}a\right)_{VOC}$ value by enhancing the contact between the gas and the NAP. Model simulations also indicated that TPPB performance can be improved by selecting: (i) adequate operational conditions (ϕ_{NAP} values $\geq$ 10%), (ii) a NAP exhibiting high affinity towards the target VOC ($K_{G/NAP}^{VOC}$ values << 1) and (iii) microorganisms with K_S < 5 g m^{-3}. The model validation with experimental RE data showed that model predictions can be drastically improved if VOC uptake in the NAP is considered. This key result was in agreement with recent works reporting the occurrence of VOC and O_2 uptake directly from the NAP. To the best of our knowledge, this is the first modeling platform for TPPBs considering continuous aqueous phase renewal and validated with experimental data from literature for three VOCs without parameter fitting. The experimental determination of the $\left(k_L^{i/j}a\right)_{VOC}$ values for several VOCs was identified as a critical research niche. Moreover, research efforts to determine experimentally X_{NAP} and kinetic parameters such as K_O and $Y_{X/O2}$ for VOC-degrading microorganisms will certainly improve model predictions and allow for a reliable model-based TPPB optimization.

Nomenclature

C_i	VOC concentration in the *i* phase (g m^{-3})
C_{Gin}	VOC concentration in air entering the TPPB (g m^{-3})
O_{2i}	O_2 concentration in the *i* phase (g m^{-3})
O_{2Win}	O_2 equilibrium concentration between air and water (8 g m^{-3})

O_{2Gin}	O_2 concentration in air entering the TPPB (250 g m^{-3})
X_i	Biomass concentration in the *i* phase (g m^{-3})
F	Gas flow rate (m^3 h^{-1})
Q	Water flow rate (m^3 h^{-1})
Q_N	NAP purge flow (m^3 h^{-1})
$K_{i/j}^{VOC}$	VOC partition coefficient between the *i* and *j* phases (m_j^3 m_i^{-3}). When *i* and *j* are the gaseous and aqueous phases, respectively, $K_{i/j}^{VOC}$ represents the dimensionless Henry's law constant of the VOC.
$K_{i/j}^{O_2}$	O_2 partition coefficient between the *i* and *j* phases (m_j^3 m_i^{-3}). When *i* and *j* are the gaseous and aqueous phases, respectively, $K_{i/j}^{O_2}$ represents the dimensionless Henry's law constant of O_2.
$\left(k_L^{i/j}a\right)_{VOC}$	Partial VOC mass transfer coefficient from the *i* to the *j* phase (h^{-1})
$\left(k_L^{i/j}a\right)_{O2}$	Partial O_2 mass transfer coefficient from the *i* to the *j* phase (h^{-1})
K_s	VOC half-saturation constant (g m^{-3})
K_O	O_2 half-saturation constant (g m^{-3})
$Y_{X/S}$	Biomass-to-VOC yield (gX $gVOC^{-1}$)
$Y_{X/O2}$	Biomass-to-O_2 yield (gX gO_2^{-1})
V_m	Molecular volume at the boiling point for VOC or O_2 (mL mol^{-1})
V_T	Total working volume of the TPPB (m^3)
X_i	Biomass concentration in the *i* phase (g m^{-3})
Greek letters	
μ_i	Specific growth rate of the microorganisms in the *i* phase (h^{-1})
μ_{max}	Maximum specific growth rate of the microorganisms (h^{-1})
μ_d	Specific decay rate of the microorganisms (h^{-1})
ϕ_i	Volume fraction of the *i* phase relative to the total working volume of the TPPB (m_i^3 m_{tot}^{-3})
Subscripts	
G	Gaseous phase
W	Aqueous phase

NAP	Non-aqueous phase

Acknowledgements

This work was financially supported by the Spanish Ministry of Economy and Competitiveness (projects DPI2011-28262-C04, CTM2012-37927-C03/FEDER, CTQ2012-34949/FEDER and contract JCI-2011-11009).

References

[1] N.J.R. Kraakman, J. Rocha-Rios, M. van Loosdrecht, Review of mass transfer aspects for biological gas treatment, Appl. Microbiol. Biotechnol. 91 (2011) 873-886.

[2] A.J. Daugulis, Two-phase partitioning bioreactors: a new technology platform for destroying xenobiotics, Trends Biotechnol. 19 (2001) 457-462.

[3] R. Muñoz, S. Villaverde, B. Guieysse, S. Revah, Two-phase partitioning bioreactors for treatment of volatile organic compounds, Biotechnol. Adv. 25 (2007) 410-422.

[4] G. Quijano, M. Hernandez, F. Thalasso, R. Muñoz, S. Villaverde, Two-phase partitioning bioreactors in environmental biotechnology, Appl. Microbiol. Biotechnol. 84 (2009) 829–846.

[5] R. Muñoz, A.J. Daugulis, M. Hernandez, G. Quijano, Recent advances in two-phase partitioning bioreactors for the treatment of volatile organic compounds, Biotechnol. Adv. 30 (2012) 1707-1720.

[6] E. Dumont, Y. Andres, P. Le Cloirec, Effect of organic solvents on oxygen mass transfer in multiphase systems: application to bioreactors in environmental protection, Biochem. Eng. J. 30 (2006) 245-252.

[7] M. Montes, M.C. Veiga, C. Kennes, Two-liquid-phase mesophilic and thermophilic biotrickling filters for the biodegradation of α-pinene, Bioresource Technol. 101 (2010) 9493-9499.

[8] H. Fam, A.J. Daugulis, Two-phase partitioning bioreactors, in: C. Kennes, M.C. Veiga (Eds.), Air Pollution Prevention and Control: Bioreactors and Bioenergy, John Wiley & Sons, Chichester, 2013, pp 185-200.

[9] S.M. Cruickshank, A.J. Daugulis, P.J. McLellan, Dynamic modeling and optimal fed-batch feeding strategies for a two-phase partitioning bioreactor, Biotechnol. Bioeng. 67 (2000) 224-33.

[10] M.H. Fazaelipoor, A model for treating air streams in a continuous two liquid phase stirred tank bioreactor, J. Hazard. Mater. 148 (2007) 453-458.

[11] D.R. Nielsen, A.J. Daugulis, P.J. McLellan, Dynamic simulation of benzene vapor treatment by a two-phase partitioning bioscrubber Part I: Model development, parameter estimation, and parametric sensitivity, Biochem. Eng. J. 36 (2007) 239-249.

[12] D.R. Nielsen, A.J. Daugulis, P.J. McLellan, Dynamic simulation of benzene vapor treatment by a two-phase partitioning bioscrubber Part II: Model calibration, validation, and predictions, Biochem. Eng. J. 36 (2007) 250-261.

[13] E. Dumont, G. Darracq, A. Couvert, C. Couriol, A. Amrane, D. Thomas, Y. Andres, P. Le Cloirec, Determination of partition coefficients of three volatile organic compounds (dimethylsulphide, dimethyldisulphide and toluene) in water/silicone oil mixtures, Chem. Eng. J. 162 (2010) 927-934.

[14] E. Dumont, G. Darracq, A. Couvert, C. Couriol, A. Amrane, D. Thomas, Y. Andres, P. Le Cloirec, VOC absorption in a countercurrent packed-bed column using water/silicone oil mixtures: influence of silicone oil volume fraction, Chem. Eng. J. 168 (2011) 241-248.

[15] J.V. Littlejohns, K.B. AcAuley, A.J. Daugulis, Model for a solid–liquid stirred tank two-phase partitioning bioscrubber for the treatment of BTEX, J. Hazard. Mater. 175 (2010) 872–882.

[16] M. Hernandez, G. Quijano, R. Muñoz, The key role of microbial characteristics on the performance of VOC biodegradation in two-liquid phase bioreactors, Environ. Sci. Technol. 46 (2012) 4059-4066.

[17] R. Muñoz, E.I.H.H Gan, M. Hernandez, G. Quijano, Hexane biodegradation in two-liquid phase bioreactors: high-performance operation based on the use of hydrophobic biomass, Biochem. Eng. J. 70 (2013) 9-16.

[18] G. Quijano, S. Revah, M. Gutierrez-Rojas, L.B. Flores-Cotera, F. Thalasso, Oxygen transfer in three-phase airlift and stirred tank reactors using silicone oil as transfer vector, Process Biochem. 44 (2009) 619-624.

[19] G. Darracq, A. Couvert, C. Couriol, A. Amrane, D. Thomas, E. Dumont, Y. Andres, P. Le Cloirec, Silicone oil: an effective absorbent for the removal of hydrophobic volatile organic compounds, J. Chem. Technol. Biotechnol. 85 (2010) 309-313.

[20] G. Quijano, M. Hernandez, S. Villaverde, F. Thalasso, R. Muñoz, A step-forward in the characterization and potential applications of solid and liquid oxygen transfer vectors, Appl. Microbiol. Biotechnol. 85 (2010) 543-551.

[21] I.Y. Smets, J.V. Haegebaert, R. Carrette, J.F. Van Impe, Linearization of the activated sludge model ASM1 for fast and reliable predictions, Water Res. 37 (2003) 1831-1851.

[22] S. Arriaga, R. Muñoz, S. Hernandez, B. Guieysse, S. Revah, Gaseous hexane biodegradation by *Fusarium solani* in two liquid phase packed-bed and stirred-tank bioreactors, Environ. Sci. Technol. 40 (2006) 2390-2395.

[23] J. Rocha-Rios, S. Bordel, S. Hernandez, S. Revah, Methane degradation in two-phase partition bioreactors, Chem. Eng. J. 152 (2009) 289-292.

[24] J.W. van Groenestijn, M.E. Lake, Elimination of alkanes from off-gases using biotrickling filters containing two liquid phases, Environ. Prog. 18 (1999) 151-155.

[25] J. Bailey, D. Ollis, Biochemical Engineering Fundamentals, 2nd ed., McGraw Hill, New York, 1986.

[26] S.J. Hwang, H.M. Tang, W.C. Wang, Modeling of acetone biofiltration process. Environ. Prog. 1997, 16 (3), 187-192.

[27] R.E. Hammervold, T.J. Overcamp, C.P.L Grady, B.F. Smets, A sorptive slurry bioscrubber for the control of acetone, J. Air Waste Manage. 50 (2000) 954-960.

[28] G. Alagappan, R.M. Cowan, Effect of temperature and dissolved oxygen on the growth kinetics of *Pseudomonas putida* F1 growing on benzene and toluene, Chemosphere 54 (2004) 1255-1265.

[29] S. Bordel, R. Muñoz, L.F. Diaz, S. Villaverde, New insights on toluene biodegradation by *Pseudomonas putida* F1: influence of pollutant concentration and excreted metabolites, Appl. Microbiol. Biotechnol. 74 (2007) 857-866.

[30] R.M.M Diks, S.P.P Ottengraf, A.H.C van den Oever, The influence of NaCl on the degradation rate of dichloromethane by *Hyphomicrobium* sp, Biodegradation 5 (1994) 129-141.

[31] M.C. Delhomenie, J. Nikiema, L. Bibeau, M. Heitz, A new method to determine the microbial kinetic parameters in biological air filters, Chem. Eng. Sci. 63 (2008) 4126-4134.

[32] M. Hernandez, J. Gouveia, G. Quijano, F. Thalasso, S. Villaverde, R. Muñoz, A systematic study of the influence on microbial kinetics of the presence of an organic phase during microbial isolation, Chem. Eng. Trans. 23 (2010) 375-380.

[33] A. Abdel-Megeed, Psychrophilic degradation of long chain alkanes, Ph.D. Dissertation, Hamburg University of Technology, Hamburg, 2004.

[34] D. Bir, Partition coefficient calculation of selected terpenes and low molecular weight solvents between tall oil fatty acid and air and polydimethyl siloxane oil and air, J. Am. Oil Chem. Soc. 77 (2000) 163-169.

[35] L. Bailon, M. Nikolausz, M. Kastner, M.C. Veiga, C. Kennes, Removal of dichloromethane from waste gases in one- and two-liquid-phase stirred tank bioreactors and biotrickling filters, Water Res. 43 (2009) 11-20.

[36] G. Darracq, A. Couvert, C. Couriol, A. Amrane, P. Le Cloirec, Kinetics of toluene and sulfur compounds removal by means of an integrated process involving the coupling of absorption and biodegradation, J. Chem. Technol. Biotechnol. 85 (2010) 1156-1161.

[37] M. Hernandez, G. Quijano, F. Thalasso, A.J. Daugulis, S. Villaverde, R. Muñoz, A comparative study of solid and liquid non-aqueous phases for the biodegradation of hexane in two-phase partitioning bioreactors, Biotechnol. Bioeng. 106 (2010) 731-740.

[38] J. Rocha-Rios, G. Quijano, F. Thalasso, S. Revah, R. Muñoz, Methane biodegradation in a two-phase partition internal loop airlift reactor with gas recirculation, J. Chem. Technol. Biotechnol. 86 (2011) 353-360.

[39] R. Sander, Compilation of Henry's Law Constants for Inorganic and Organic Species of Potential Importance in Environmental Chemistry, 1999, http://www.mpch-mainz.mpg.de/~sander/res/henry.html.

[40] Y. Yu, J.A. Ramsay, B.A. Ramsay, On-line estimation of dissolved methane concentration during methanotrophic fermentations, Biotechnol. Bioeng. 95 (2006) 788-793.

[41] C.R. Wilke, P. Chang, Correlation of diffusion coefficients in dilute solutions, AIChE J. 1 (1955) 264-270.

[42] C. McAuliffe, Solubility in water of paraffin, cycloparaffin, olefin, acetylene, cycloolefin, and aromatic hydrocarbons, J. Phys. Chem. 70 (1966) 1267-1275.

[43] A. Gavezzotti, The calculation of molecular volumes and the use of volume analysis in the investigation of structured media and of solid-state organic reactivity, J. Am. Chem. Soc. 105 (1983) 5220-5225.

[44] C.E. Webster, R.S. Drago, M.C. Zerner, Molecular dimensions for adsorptives, J. Am. Chem. Soc. 120 (1998) 5509-5516.

[45] J.M. Estrada, A. Dudek, R. Muñoz, G. Quijano, Fundamental study on gas-liquid mass transfer in a biotrickling filter packed with polyurethane foam, J. Chem. Technol. Biotechnol. DOI: 10.1002/jctb.4226.

[46] R. Muñoz, S. Arriaga, S. Hernandez, B. Guieysse, S. Revah, Enhanced hexane biodegradation in a two phase partitioning bioreactor: overcoming pollutant transport limitations, Process Biochem. 41 (2006) 1614–1619.

[47] E. Dumont, H. Delmas, Mass transfer enhancement of gas absorption in oil-in-water systems: a review, Chem. Eng. Process. 42 (2003) 419-438.

[48] M.T. Cesario, H.H. Beeftink, J. Tramper, Feasibility of using water-immiscible in biological waste-gas treatment, Bioprocess Eng. 12 (1995) 55-63.

[49] R. Muñoz, M. Chambaud, S. Bordel, S. Villaverde, A systematic selection of the non-aqueous phase in a bacterial two liquid phase bioreactor treating α-pinene, Appl. Microbiol. Biotechnol. 79 (2008) 33-41.

Figure captions

Fig. 1. Model predicted (white bars) and experimental (black bars) RE values for: (A) control reactors without NAP, (B) TPPBs without VOC uptake in the NAP and (C) TPPBs assuming VOC uptake in the NAP. The experimental conditions set in each work are summarized in Table 4.

Fig. 2. Experimental (black bars) and model predicted RE values increasing 30% (white bars) and 50% (lined bars) the $\left(k_L^{G/NAP}a\right)_{VOC}$ coefficient relative to the initial value given in Table 5.

Fig. 3. Model sensitivity analysis expressed as the effect on the RE predicted by the model for a relative parameter variation. It has been classified in (A) operational, (B) mass transfer, (C) partition and (D) kinetic terms.

Figure captions

Fig. 1. Model predicted (white bars) and experimental (black bars) RE values for: (A) control reactors without NAP, (B) TPPBs without VOC uptake in the NAP and (C) TPPBs assuming VOC uptake in the NAP. The experimental conditions set in each work are summarized in Table 4.

Fig. 2. Experimental (black bars) and model predicted RE values increasing 30% (white bars) and 50% (lined bars) the $\left(k_L^{G/NAP}a\right)_{VOC}$ coefficient relative to the initial value given in Table 5.

Fig. 3. Model sensitivity analysis expressed as the effect on the RE predicted by the model for a relative parameter variation. The sensitivity analysis was performed for (A) operational, (B) mass transfer, (C) partition and (D) kinetic parameters.

Table 1. Kinetic and stoichiometric parameters of VOC-degrading microorganisms obtained at 25ºC.

VOC	**Microorganism**	**μ_{max} (h^{-1})**	**Ks ($g\ m^{-3}$)**	**K_O ($g\ m^{-3}$)**	**$Y_{X/S}$ ($g\ g^{-1}$)**	**$Y_{X/O2}$ ($g\ g^{-1}$)**	**Reference**
Acetone	Mixed microbial consortium contained in compost	0.036	10.33	0.5	0.25	0.23	[26]
Acetone	Mixed bacterial consortium	0.37	1.45	-	0.33	-	[27]
Toluene	*Pseudomonas putida* F1	0.42	2.50	1.1	0.65	-	[28]
Toluene	*Pseudomonas putida* F1	0.78	5	-	1.08	-	[29]
Dichloromethane	*Hyphomicrobium sp.*	0.08	8.5	-	0.18	-	[30]
Methane	*Methylocystis parvus*	0.045	7.59	-	0.57	-	[31]
Hexane	*Pseudomonas aeruginosa*	0.20	0.26	-	-	-	[32]
Hexane	*Pseudomonas putida*	-	-	-	1.17	-	[33]

Table 2. Partition parameters for target VOCs and O_2 at 25°C.

Gaseous substrate	$\mathbf{K_{G/W}}$[a]	$\mathbf{K_{G/NAP}}$	$\mathbf{K_{NAP/W}}$[b]	**Reference**
Acetone	0.0014	191	7.32×10^{-6}	[34]
Dichloromethane	0.11	0.07	1.57	[35]
Toluene	0.27	0.00064	422	[36]
Hexane	70	0.0058	12000	[37]
O_2	30	3.6	8.3	[20]
Methane	31	1.8	17.2	[38]

[a]Dimensionless Henry's law constant value. Data from Sander [39].

[b]Calculated as: $\frac{K_{G/W}}{K_{G/NAP}}$

Table

Table 3. Mass transfer parameters experimentally determined for O_2 and estimated for VOCs at several NAP fractions

Experimental mass transfer coefficients for O_2 (h^{-1})[a]				**Estimated mass transfer coefficients for VOCs (h^{-1})[b]**			
NAP %(v/v)	$\left(k_L^{G/W}a\right)_{O_2}$	$\left(k_L^{G/NAP}a\right)_{O_2}$	$\left(k_L^{NAP/W}a\right)_{O_2}$	**VOC**	$\left(k_L^{G/W}a\right)_{VOC}$	$\left(k_L^{G/NAP}a\right)_{VOC}$	$\left(k_L^{NAP/W}a\right)_{VOC}$
0	109	-	-	Acetone	73	-	-
				Toluene	61	-	-
				Hexane	57	-	-
				Dichloromethane	81	-	-
				Methane	93	-	-
5	176	0.47	13	Acetone	117	0.3	9.0
				Toluene	98	0.3	7.2
				Hexane	92	0.2	6.8
				Dichloromethane	130	0.3	10.0
				Methane	150	0.4	11.1
10	187	1.89	72	Acetone	125	1.3	48
				Toluene	104	1.1	40
				Hexane	97	1.0	38
				Dichloromethane	139	1.4	53
				Methane	160	1.6	62
20	109	5.54	210	Acetone	73	3.7	140
				Toluene	61	3.1	117
				Hexane	57	2.9	109
				Dichloromethane	81	4.1	156
				Methane	93	4.7	180
50	70	8.46	1315	Acetone	47	5.6	877
				Toluene	39	4.7	731
				Hexane	36	4.4	685
				Dichloromethane	52	6.3	974
				Methane	60	7.2	1125

[a]Mass transfer coefficients reported by Quijano et al. [18]

[b]Estimated using Equation 12.

Table 4. Experimental studies on VOC removal in TPPBs operated as stirred tanks using silicone oil as a NAP.

VOC	Experimental conditions[a]	Microorganisms	Experimental time (days)	C_{Gin} (g m^{-3})	VOC loading rate (g m^3 h^{-1})	Removal efficiency (%)[b]	Biomass in the NAP	Reference
Dichloro-methane	V_T=1.5 × 10^{-3} m^3 Agitation rate = 400 rpm T= 30°C F= 0.084 m^3 h^{-1} Water renewal: Yes Q= not specified Gas residence time = 1.07 min NAP addition = 10% v/v	Mixed microbial community containing *Hyphomicrobium* KDM2 and KDM4	250	1.8	100	90% (control without NAP)	-	Bailon et al. [35] (case A)
						100% (TPPB)	No	
				5.3	300	25% (control without NAP)	-	Bailon et al. [35] (case B)
						95% (TPPB)	No	
Hexane	V_T=2 × 10^{-3} m^3 Agitation rate = 300 rpm T= 30°C F= 0.06 m^3 h^{-1} Water renewal: Yes Q= 5.8 × 10^{-5} m^3 h^{-1} Gas residence time = 2.00 min NAP addition= 20% v/v	Mixed bacterial community	25	2.1	64	5.7% (control without NAP)	-	Hernandez et al. [16]
						50% (TPPB)	No	
						90% (TPPB)	Yes	
Hexane	V_T=2.25 × 10^{-3} m^3 Agitation rate = 300 rpm T= 25°C F= 0.12 m^3 h^{-1} Water renewal: Yes Q= 1.87 × 10^{-5} m^3 h^{-1} Gas residence time = 1.10 min NAP addition= 10% v/v	Mixed bacterial community isolated from a wastewater treatment plant	80	0.5	24	4.4% (control without NAP)	-	Muñoz et al. [17]
						80% (TPPB)	Yes	
Methane	V_T=2 × 10^{-3} m^3 Agitation rate = 800 rpm T= 30°C F= 0.025 m^3 h^{-1} Water renewal: Yes Q= 8.3 x 10^{-6} m^3 h^{-1} Gas residence time = 4.70 min NAP addition= 10% v/v	Methanotrophic consortium isolated from a wastewater treatment plant	Not specified	11.1	200	34% (control without NAP)	-	Rocha-Rios et al. [23]
						57% (TPPB)	No	
Hexane	V_T=1.5 × 10^{-3} m^3 Agitation rate = 400 rpm T= 30°C F= 0.09 m^3 h^{-1} Water renewal: Yes Q= 2.0 × 10^{-6} m^3 h^{-1} Gas residence time = 1.00 min NAP addition = 10% v/v	*Pseudomonas aeruginosa*	8	3	180	10% (control without NAP)	-	Muñoz et al. [46]
						42% (TPPB)	No	

[a]When the value of Q was not specified, the minimum value reported in the literature (2 x 10^{-6} m^3 h^{-1}) was assumed.

[b]Average stable values were considered.

Table 5. Initial values for the parameters in the sensitivity analysis using toluene as the reference VOC.

Parameter	**Initial Value**
V_T	0.01 m^3
F	0.6 $m^3\ h^{-1}$
Q	3 x 10^{-5} $m^3\ h^{-1}$
$C_{G\text{in}}$	1 g m^{-3}
$O_{2G\text{in}}$	250 g m^{-3}
ϕ_W	0.8 $m_W^3\ m_{tot}^{-3}$
ϕ_{NAP}	0.1 $m_{NAP}^3\ m_{tot}^{-3}$
ϕ_G	0.1 $m_G^3\ m_{tot}^{-3}$
$\left(k_L^{G/W}a\right)_{VOC}$	104 h^{-1}
$\left(k_L^{G/NAP}a\right)_{VOC}$	1.1 h^{-1}
$\left(k_L^{NAP/W}a\right)_{VOC}$	40 h^{-1}
$\left(k_L^{G/W}a\right)_{O2}$	187 h^{-1}
$\left(k_L^{G/NAP}a\right)_{O2}$	1.89 h^{-1}
$\left(k_L^{NAP/W}a\right)_{O2}$	72 h^{-1}
$K_{G/W}^{VOC}$	0.27 $h^{-1}\ m_W^3\ m_G^{-3}$
$K_{G/NAP}^{VOC}$	0.00064 $m_{NAP}^3\ m_G^{-3}$
$K_{NAP/W}^{VOC}$	422 $m_W^3\ m_{NAP}^{-3}$
$K_{G/W}^{O_2}$	30 $m_W^3\ m_G^{-3}$
$K_{G/NAP}^{O_2}$	3.6 $m_{NAP}^3\ m_G^{-3}$
$K_{NAP/W}^{O_2}$	8.3 $m_W^3\ m_{NAP}^{-3}$
μ_{max}	0.25 h^{-1}
μ_d	0.025 h^{-1}
K_s	5 g m^{-3}
K_O	0.7 g m^{-3}
$Y_{X/S}$	0.3 g g^{-1}
$Y_{X/O2}$	0.4 g g^{-1}

Figure

Fig. 1

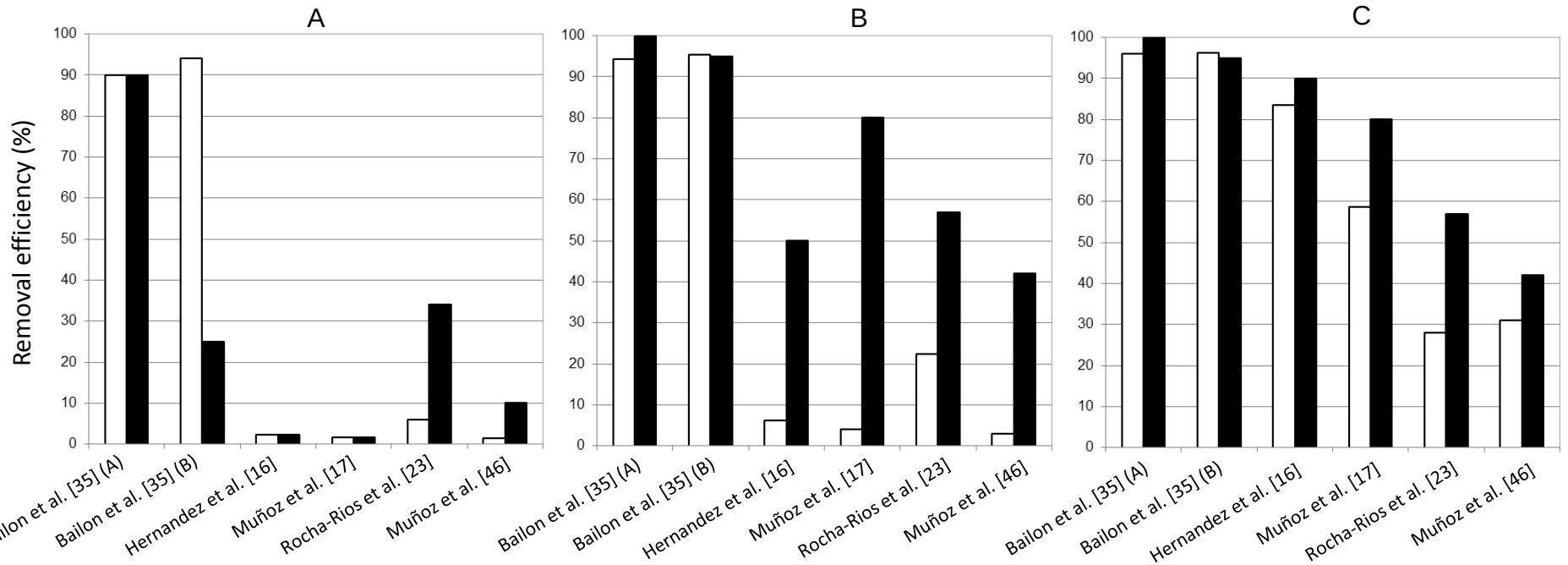
A
B
C
Removal efficiency (%)
0
10
20
30
40
50
60
70
80
90
100
Bailon et al. [35] (A)
Bailon et al. [35] (B)
Hernandez et al. [16]
Muñoz et al. [17]
Rocha-Rios et al. [23]
Muñoz et al. [46]

Figure

Fig. 2

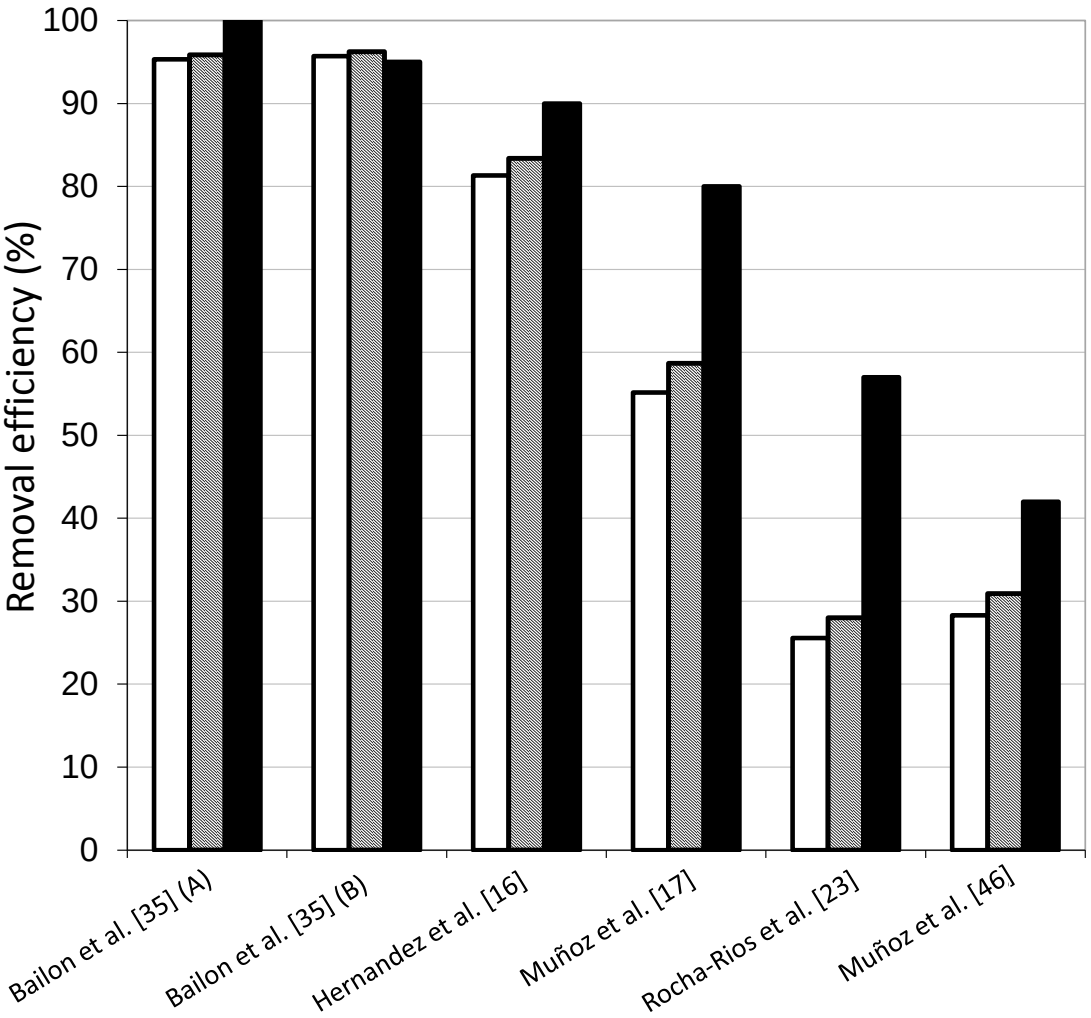
Removal efficiency (%)
100
90
80
70
60
50
40
30
20
10
0
Bailon et al. [35] (A)
Bailon et al. [35] (B)
Hernandez et al. [16]
Muñoz et al. [17]
Rocha-Rios et al. [23]
Muñoz et al. [46]

Figure

Fig. 3.

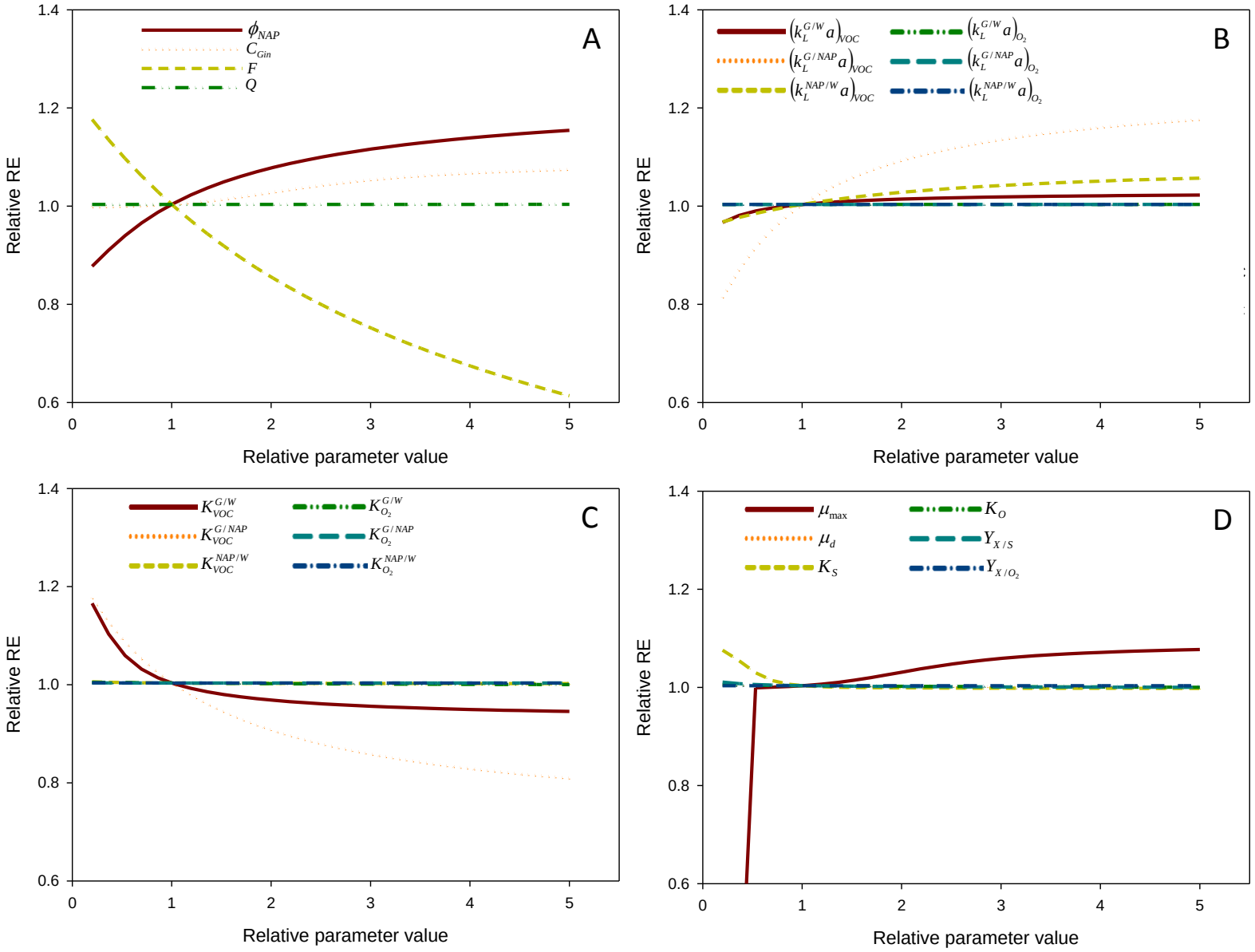
A
B
C
D
Relative RE
Relative parameter value
ϕ_{NAP}
C_{Gin}
F
Q
$\left(k_L^{G/W}a\right)_{VOC}$
$\left(k_L^{G/W}a\right)_{O_2}$
$\left(k_L^{G/NAP}a\right)_{VOC}$
$\left(k_L^{G/NAP}a\right)_{O_2}$
$\left(k_L^{NAP/W}a\right)_{VOC}$
$\left(k_L^{NAP/W}a\right)_{O_2}$
$K_{VOC}^{G/W}$
$K_{O_2}^{G/W}$
$K_{VOC}^{G/NAP}$
$K_{O_2}^{G/NAP}$
$K_{VOC}^{NAP/W}$
$K_{O_2}^{NAP/W}$
μ_{max}
K_O
μ_d
$Y_{X/S}$
K_S
Y_{X/O_2}